Received: 2 October 2017 | Revised: 15 November 2017 | Accepted: 17 November 2017

DOI: 10.1111/cas.13453

ORIGINAL ARTICLE

WILEY Cancer Science

HOXC13 promotes proliferation of esophageal squamous cell carcinoma via repressing transcription of CASP3

Jing Luo[1,2] | Zhongqiu Wang[2,3] | Jianfeng Huang[2,3] | Yu Yao[4] | Qi Sun[1,2] | Jie Wang[2] | Yi Shen[1] | Lin Xu[2,3] | Binhui Ren[2,3]

[1]Department of Cardiothoracic Surgery, Jinling Hospital, Medical School of Nanjing University, Nanjing, China

[2]Jiangsu Key Laboratory of Molecular and Translational Cancer Research, Nanjing, China

[3]Department of Thoracic Surgery, Jiangsu Cancer Hospital, Cancer Institute of Jiangsu Province, Institute Affiliated to Nanjing Medical University, Nanjing, China

[4]Department of Respiratory Medicine, Nanjing Chest Hospital, Medical School of Southeast University, Nanjing, China

Correspondence
Yi Shen, Department of Cardiothoracic Surgery, Jinling Hospital, Medical School of Nanjing University, Nanjing, China.
Email: shenyi1599623@163.com
and
Lin Xu, Binhui Ren, Department of Thoracic Surgery, Jiangsu Cancer Hospital, Institute Affiliated to Nanjing Medical University, Cancer Institute of Jiangsu Province, Nanjing, China.
Emails: xulin83z@163.com; robbishren@163.com

Funding information
National Natural Science Foundation of China (81172032); Jiangsu Provincial Special Program of Medical Science Funding (BL2012030); Jiangsu Provincial Science Foundation (BK20161596); Jiangsu Provincial Medical Outstanding Talent (Lin Xu); Jiangsu Provincial Medical Youth Talent (Binhui Ren, QNRC2016657); Jiangsu Provincial key research development program (BE2017758).

Esophageal squamous cell carcinoma (ESCC), the dominant subtype of esophageal cancer, is one of the most common digestive tumors worldwide. In this study, we confirmed that HOXC13, a member of the homeobox HOXC gene family, was significantly upregulated in ESCC and its overexpression was associated with poorer clinical characteristics and worse prognosis. Moreover, knockdown of HOXC13 inhibited proliferation and induced apoptosis of ESCC through upregulating CASP3. ChIP analysis revealed that HOXC13 repressed transcription of CASP3 through directly targeting the promotor region of CASP3. We also found that miR-503 downregulated HOXC13, by directly targeting its 3′UTR, and inhibited proliferation of ESCC. In conclusion, our study demonstrates that HOXC13, which is directly targeted by miR-503, promotes proliferation and inhibits apoptosis of ESCC through repressing transcription of CASP3.

KEYWORDS
apoptosis, CASP3, esophageal squamous cell carcinoma, HOXC13, miR-503

1 | INTRODUCTION

Esophageal cancer, the sixth leading cause of cancer death in the world,[1] is one of the most aggressive and lethal digestive tract tumors. Esophageal squamous cell carcinoma (ESCC) is the dominant subtype of esophageal cancer and accounts for 90% of diagnosed esophageal cancer.[2] Although there have been improvements in diagnosis and treatment of ESCC, the overall 5-year survival rate is less than 25% due to diagnosis in later stages accompanied by local invasion and distant metastasis.[3] Therefore,

Jing Luo, Zhongqiu Wang and Jianfeng Huang contributed equally to this work.

seeking new functional genes and biomarkers in ESCC development may yield alternative approaches for managing esophageal cancer.

As known, HOX genes are a group of related genes containing a well-conserved DNA sequence called the homeobox.[4] The protein products of HOX genes function as transcription factors that bind to specific nucleotide sequences on the DNA called enhancers where they either activate or repress genes.[5] As a member of the homeobox HOXC gene family, HOXC13 correlates with the development of hair, nail and filiform papilla.[6-8] It has been reported that HOXC13 is highly expressed in ameloblastoma,[9] odontogenic tumors,[10] metastatic melanoma[11] and liposarcoma;[12] moreover, knockdown of HOXC13 inhibited cell growth, and resulted in cell cycle arrest, in colon cancer.[13] However, the expression and biological function of HOXC13 in ESCC have not been investigated. In this study, we confirmed that HOXC13 could play an oncogenic role in ESCC through repressing transcription of CASP3.

MicroRNA (miRNA) are a class of small non-coding RNA molecules that regulate gene expression at post-transcriptional level.[14] They bind to the 3′ untranslated regions (3′UTR) of target genes, and regulate the translation and degradation of target mRNA.[15] MicroRNA play important roles in multiple physiological processes, including developmental timing, cell death and proliferation, hematopoiesis, and progression of many kinds of human cancers.[16-19] Plenty of miRNA have been reported to be related to tumor proliferation and patient survival in ESCC.[20-23] Technologies aimed at replacing tumor suppressor miRNA that are lost during cancer progression have emerged as promising cancer therapies.[24] Herein, we show that miR-503 targets the 3′UTR of HOXC13 and represses proliferation of ESCC. Further study of the role of miR-503-HOXC13-CASP3 axis in ESCC initiation and development is expected to provide new biomarkers and therapeutic targets for ESCC.

2 | MATERIALS AND METHODS

2.1 | Data sources and bioinformatics

The TCGA dataset, named TCGA_ESCA_exp_HiSeq-2015-02-24, was downloaded from the UCSC Cancer Browser (https://genome-cancer.ucsc.edu/).[25] All normalized gene expression values can be obtained from "genomicMatrix" files. Using the co-expression tool in cBioPortal (http://www.cbioportal.org/),[26] we obtained a list of 120 genes (Table S1) with high co-expression correlation (Pearson score >0.38) with HOXC13. These genes were submitted to DAVID Bioinformatics Resources 6.8 (http://david.abcc.ncifcrf.gov/)[27] for Gene Ontology (GO) pathway analysis. To predict the binding site of HOXC13 with the promotor region of CASP3, the Jaspar Database (http://jaspar.genereg.net/)[28] was used. The mirSVR predicted target site scoring method (http://www.microrna.org/microrna/home.do)[29] was used to search for miRNA that directly target 3′UTR of HOXC13.

2.2 | Tissue samples and animal studies

In total, 60 ESCC tissue samples were obtained from patients who had undergone curative surgical resection in the department of thoracic surgery, Nanjing Jinling Hospital, from 2013 to 2016. None of the patients had received preoperative chemotherapy or radiotherapy. All patients' clinicopathological parameters, including age, gender, primary tumor size, lymph node status, TNM stage, tumor location and focus type, were obtained from their medical records.

All animal studies were conducted in accordance with NIH animal use guidelines and protocols were approved by Nanjing Medical University Animal Care Committee. Twelve female nude mice (ages 4-6 weeks) were purchased from Nanjing Medical University School of Medicine's accredited animal facility. Briefly, 1.0×10^6 exponentially growing ECA109 cells with ectopic expression of appropriate genes or miRNA were injected subcutaneously. Tumor volume was estimated using calipers every week ([length $\times$ width^2]/2). Six weeks after injection, mice were sacrificed, tumor weights were measured and tumors were collected for further analysis.

2.3 | Immunohistochemistry

Immunohistochemistry (IHC) for HOXC13 and CASP3 protein expression in samples was performed using standard methods. Tissue sections were deparaffinized and rehydrated through graded alcohol. Endogenous peroxidase activity was blocked by incubation in 3% H_2O_2. Antigen retrieval was carried out with 0.01 mol/L citrate buffer (pH 6.0) and microwave heat induction. Anti-HOXC13 mouse monoclonal antibody (Abcam, Cambridge, UK; ab55251) and anti-CASP3 rabbit polyclonal antibody (Abnova, Taibei, Taiwan; PAB0242) were used.

2.4 | Cell culture, Z-DEVD-FMK, shRNA, microRNA mimics and transfection

ECA109 and TE13 cells were cultured in DMEM media (KeyGEN, Nanjing, China) supplemented with 10% FBS and penicillin/streptomycin (KeyGEN), and cultured at 37°C in a humidified incubator containing 5% CO_2. Z-DEVD-FMK, a caspase-3 inhibitor, was purchased from Selleck and DMSO was used as the negative control. shRNA and microRNA mimics were conducted and purchased from Vigene Biosciences, Shandong, China. Transfection of shRNA and miR-503 mimics was performed according to the Lipofectamine 3000 Reagent (Invitrogen, Carlsbad, CA, USA) protocol; nonsense shRNA (sh-nc) and negative control mimic (miR-nc) were used as the respective controls. Transfection efficiency was evaluated by quantitative real-time RT-PCR (qRT-PCR) and western blot.

The sequences used were as follows: shRNA-1 for HOXC13, 5′-GAGCCTTATGTACGTCTATGATTCAAGAGATCATAGACGTACATAAGGCTCTTTTTT-3′; shRNA-2 for HOXC13, 5′-GCAAATCGAAAGCGCCTCATCTTCAAGAGAGATGAGGCGCTTTCGATTTGCTTTTTT-3′; sh-nc, 5′-GCACCCAGTCCGCCCTGAGCAAATTCAAGAGATTTGCTCA

GGGCGGACTGGGTGCTTTTT-3′; miR-503 mimics, 5′-GGGGUAUUG UUUCCGCUGCCAGG-3′, and miR-nc mimics, 5′-UUCUCCGAACGU GUCACGUTT-3′.

2.5 | RNA extraction, reverse transcription and quantitative RT-PCR

Total RNA was extracted from tissue samples or cultured cells using TRIzol reagent (Invitrogen) according to the manufacturer's instructions. Reverse transcription was performed with 1000 ng total RNA in a final volume of 20 μL, using a Reverse Transcription Kit (Takara, cat: RR036A, KeyGEN). For qRT-PCR, SYBR Select Master Mix (Applied Biosystems, Cat: 4472908. KeyGEN) was used, and the reaction was performed in a QuantStudio 6 Flex Real-Time PCR System as follows: initial denaturation step at 95°C for 10 minutes, followed by 40 cycles at 92°C for 15 seconds and 60°C for 1 minute. Primers are shown in Table S2 and ACTB was used as a housekeeping gene. The comparative CT method (ΔΔCT) was used to measure relative gene expression.

2.6 | Protein extracts and western blot analysis

Cells were harvested and treated with lysis buffer (RIPA, KeyGEN) on ice, and protein concentration was determined using a BCA Kit (KeyGEN). Comparable amounts of extracts were loaded on SDS–PAGE gels and subjected to electrophoresis. After separation on the gel, proteins were transferred to a PVDF membrane. Membranes were blocked in 2% BSA in TBS-T for 1 hour, and subsequently incubated overnight, at 4°C, with antibodies against HOXC13 (Santa Cruz, Dallas, TX, USA; sc-514377; 1:1000), CASP3 (Proteintech, Rosemont, IL, USA; 19677-1-AP; 1:1000), PARP (Cell Signaling Technology, Danvers, Massachusetts, USA; 9542; 1:1000) or β-actin (Cell Signaling Technology, Danvers, MA, USA; 8H10D10; 1:1000). After washing in TBS-T, membranes were incubated with goat anti-rabbit or goat anti-mouse HRP-conjugated secondary antibodies (both from Abcam; 1:10 000), for 2 hours at room temperature. Blots were visualized using ECL detection (Thermo Fisher Scientific, Waltham, MA, USA). All experiments were repeated at least three times, independently.

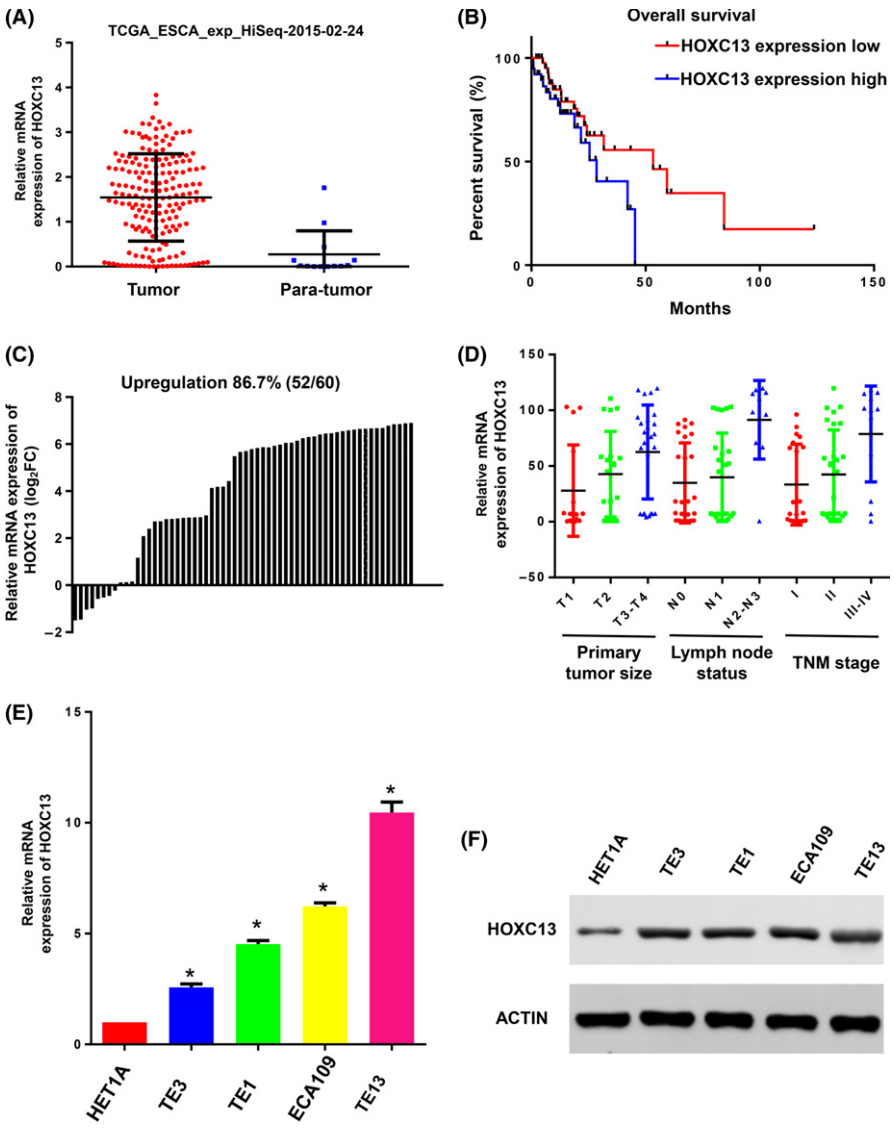

FIGURE 1 HOXC13 is generally highly expressed in esophageal squamous cell carcinoma (ESCC) tissues and correlates with poorer prognosis. A, TCGA datasets show that HOXC13 is significantly upregulated in esophageal carcinoma tissues than in para-tumor tissues ($P < .0001$). B, Esophageal carcinoma patients with low expression of HOXC13 show superior overall survival to patients with high expression of HOXC13 (median survival 1599 vs 855 d; $P = .0308$). C, Quantitative RT-PCR analysis showed that HOXC13 was upregulated in 86.7% of 60 ESCC tissues (normalized to adjacent normal tissues). D, Overexpression of HOXC13 is associated with greater T stage ($P = .0338$), N stage ($P = .0003$) and TNM stage ($P = .0062$) in ESCC patients. E,F, HOXC13 mRNA and protein are highly expressed in ESCC cell lines

2.7 | Cell Counting Kit-8, colony formation and xCELLigence System assays

The assays were performed 24 hours after transfection. For the Cell Counting Kit-8 (CCK-8) assay, cells were plated in 96-well plates at a density of 2000 cells/100 μL, and the absorbance was measured at 450 nm in an ELx-800 Universal Microplate Reader. For colony formation assay, a total of 200 cells were placed in a fresh 6-well plate and cultured in medium containing 10% FBS, with medium replacement every 3-4 days. After 2 weeks, cells were fixed with 4% paraformaldehyde and stained with 0.1% crystal violet. Visible colonies were manually counted. For the xCELLigence System, 8000 cells/100 μL were seeded in E-plates, and the plates were locked into the RTCA DP device in the incubator. The proliferative ability in each well was automatically monitored by the xCELLigence System, and expressed as a "cell index" value. All experiments were repeated at least three times.

2.8 | Assessment of apoptosis: TUNEL staining

TUNEL kits (KeyGEN BioTECH, KGA7062, China) were used to detect DNA fragmentation of apoptotic cells. After transfection, 4×10^3 cells were seeded in 24-well plates for 24 hours. Then, cells were incubated at 37°C for 1 hour with terminal deoxynucleotidyl transferase enzyme and cell nuclei were counterstained with DAPI. Images were obtained from a fluorescence microscope for further calculation of apoptosis proportion.

2.9 | Luciferase reporter assay

HEK293T cells were grown in 24-well plates using DMEM containing 10% FBS (Invitrogen). Luciferase reporter genes were then co-transfected into cells, together with the indicated expression plasmids or microRNA mimics. The Ramlila luciferase expression vector CMV-Empty or miR-nc was used as an internal control. After 48 hours, cells were harvested and assessed for luciferase activity using the Dual Luciferase Reporter Assay System (Promega, Madison, WI, USA). Relative luciferase activity was corrected for Renilla luciferase activity of CMV-Empty or miR-nc, and normalized to the activity of the control.

2.10 | ChIP assay

ECA109 cells were cross-linked in 4% paraformaldehyde and the reaction was quenched with glycine. After two washes with cold PBS, cells were scraped in 0.5 mL swelling buffer and incubated on ice for 10 minutes. Pelleted cells were resuspended in lysis buffer and incubated on ice for 10 minutes. Chromatin DNA was sonicated and centrifuged for 10 minutes at 12 000 *g* at 4°C. HOXC13 was immunoprecipitated from the cleared lysates for 2 hours with a mouse monoclonal anti-HOXC13 antibody (Santa Cruz, sc-81967) coupled to agarose beads (Resin M2, Sigma, Shanghai, China). After washing and elution, the protein–DNA complex was reversed by heating at 65°C for 4 hours. Eluate was adjusted to 40 mmol/L Tris pH 6.8, 10 mmol/L EDTA, then incubated with RNase A, and followed by proteinase K. DNA was recovered by phenol:chloroform extraction. PCR was performed with MasterMix from 5 Prime with the following primer sets:

CASP3 (Primer1) promotor, 5′-TGAGGCAGAAAAAGGACT GTCA-3′ (Forward) and 5′-GGGGTTAAGTAGTTTGCTGTTGC-3′ (Reverse); CASP3 (Primer2) promotor, 5′-TGGGAGTGGGTCCTATTTC TCA-3′ (Forward) and 5′-AGGCCTTTCTTTATCCCTCCT-3′ (Reverse); control primers, 5′-GGGAGTGGGTCCTATTTCTCA-3′ (Forward) and 5′-GGCCTTTCTTTATCCCTCCTGAA-3′ (Reverse).

2.11 | Statistical analysis

All results are presented as the mean ± SD. Student's *t*-test, χ^2-test, Cox regression analysis, Pearson test, one-way ANOVA analysis and Kaplan–Meier survival analysis were used to analyze the data using SPSS Statistics software (version 20.0, Chicago, IL, USA). $P < .05$ was considered statistically significant. Graphs were made using the GraphPad Prism 6.0 software package (La Jolla, CA, USA).

TABLE 1 Correlation between HOXC13 expression and clinical characteristics

Characteristics	Low level of HOXC13 expression number	High level of HOXC13 expression number	*P*-value
Age (years)			
≤65	21	26	.297032
>65	25	20	
Sex			
Male	40	42	.502915
Female	6	4	
Metastasis			
M0	31	35	.352308
M1–MX	15	11	
Lymph node			
N0	20	19	.16014
N1	20	14	
N2–NX	6	13	
Primary tumor			
T1	13	2	.010528*
T2	8	13	
T3	24	27	
T4	1	4	
TNM stage			
I	12	2	.031380*
II	18	20	
III	12	18	
IV	4	6	

*Significant correlation.

3 | RESULTS

3.1 | HOXC13 is highly expressed in esophageal squamous cell carcinoma tissues, and correlates with poorer prognosis and more aggressive clinical characteristics

By analyzing the TCGA_ESCA_exp_HiSeq-2015-02-24 dataset, we found that expression of HOXC13 is significantly higher in esophageal carcinoma tissues than in para-tumor tissues (Figure 1A). For the 184 cases of esophageal carcinoma tissues with clinical prognosis and TNM stage information, we interpreted cases in the upper quartile of HOXC13 expression as having "high HOXC13 expression," and cases in the lower quartile as having "low HOXC13 expression." Survival curve analysis demonstrated that patients with low expression of HOXC13 presented a higher percentage of overall survival than patients with high expression of HOXC13 (median survival 1599 vs 855 days; $P = .0308$, Figure 1B). In addition,

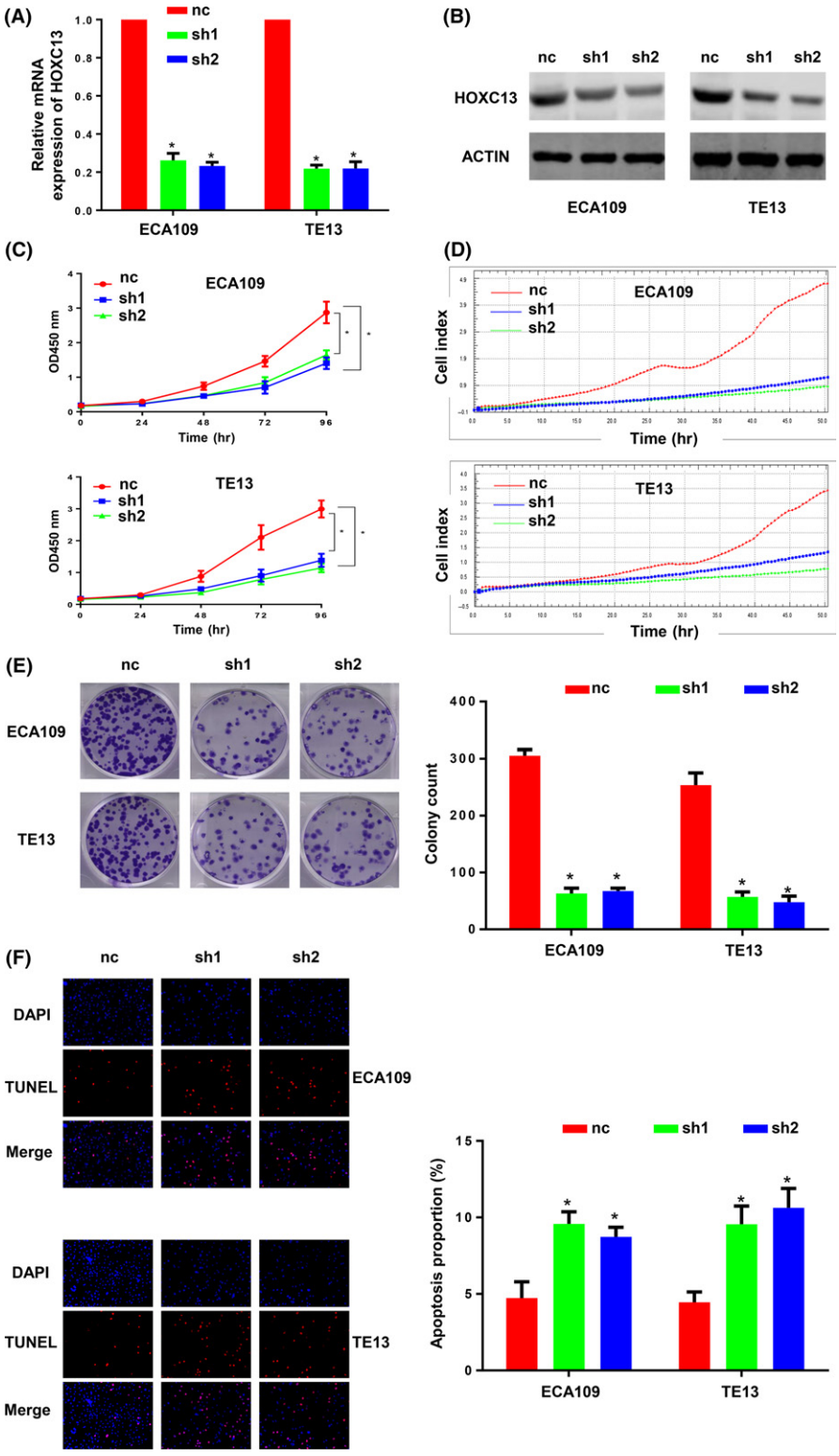

FIGURE 2 Knockdown of HOXC13 inhibits proliferation of esophageal squamous cell carcinoma (ESCC) cells and induces apoptosis. A,B, Two specific shRNA (sh1 and sh2) of HOXC13 were designed and synthesized, and the transfection efficiency in ECA109 and TE13 cells was measured by quantitative RT-PCR and western blot. C, Cell Counting Kit-8 assays revealed that knockdown of HOXC13 inhibited proliferation of ECA109 cells (sh1, $P < .0001$; sh2, $P < .0001$) and TE13 cells (sh1, $P < .0001$; sh2, $P < .0001$). D, XCELLigence System assays also showed that knockdown of HOXC13 inhibited proliferation of ECA109 cells (sh1, $P < .0001$; sh2, $P < .0001$) and TE13 cells (sh1, $P < .0001$; sh2, $P < .0001$). E, Colony formation ability was inhibited by knockdown of HOXC13 in ECA109 cells (sh1, $P = .0002$; sh2, $P = .0001$) and TE13 cells (sh1, $P = .0036$; sh2, $P = .0037$). F, Knockdown of HOXC13 induced apoptosis of ECA109 cells (sh1, $P = .0040$; sh2, $P = .0151$) and TE13 cells (sh1, $P = .0031$; sh2, $P = .0026$)

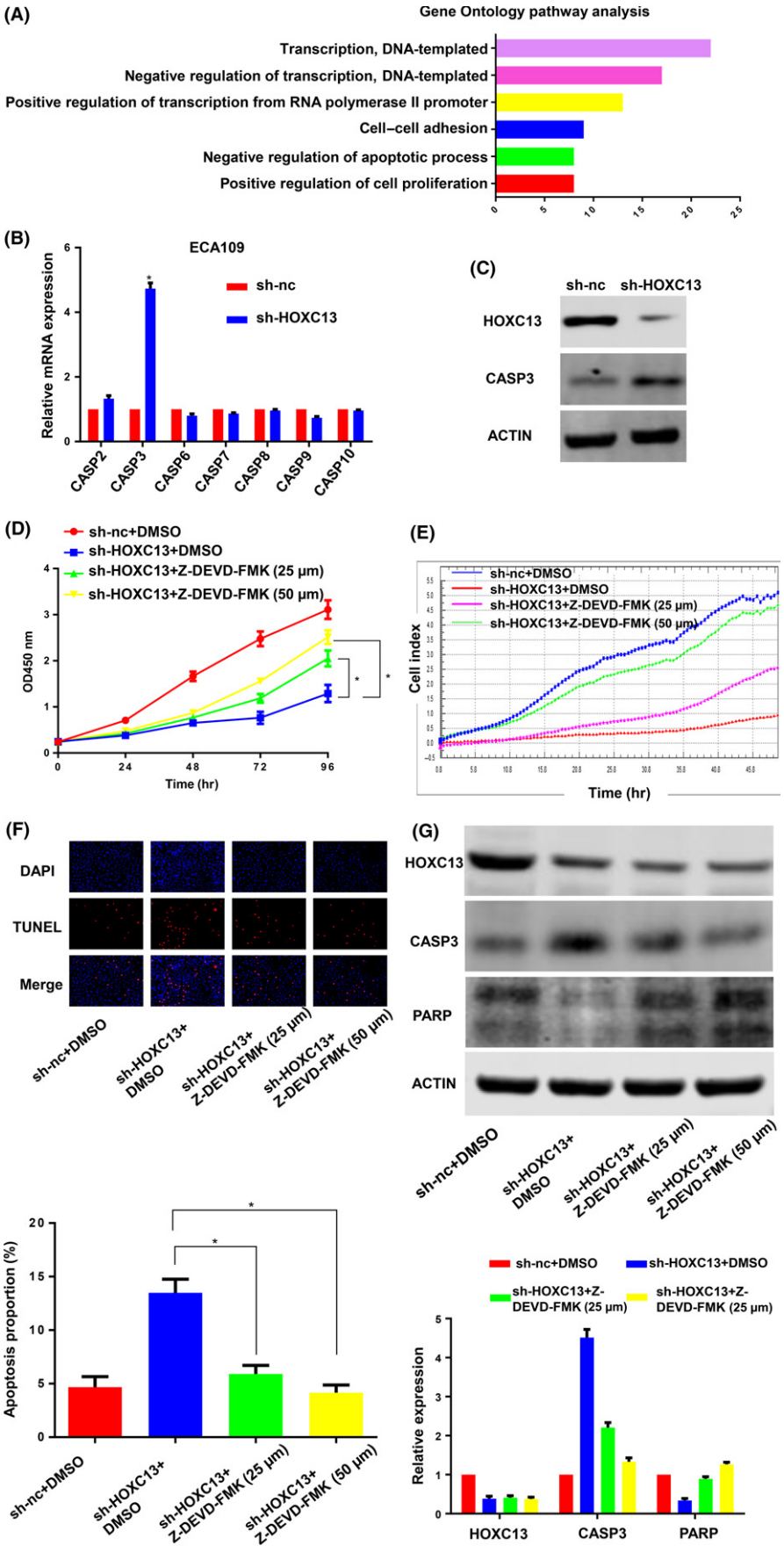

FIGURE 3 HOXC13 induces apoptosis of esophageal squamous cell carcinoma (ESCC) cells through regulating CASP3. A, Gene ontology pathway analysis showed that genes co-expressed with HOXC13 were enriched in the "transcription," "apoptotic process" and "proliferation" pathway. B,C, Quantitative RT-PCR and western blot indicated that expression of CASP3 was significantly upregulated by knockdown of HOXC13. D,E, Z-DEVD-FMK, a specific caspase-3 inhibitor, partially reversed the inhibitory effect of sh-HOXC13 on the proliferation of ECA109 cells. F, Z-DEVD-FMK partially reversed shRNA-HOXC13-induced apoptosis. G, Western blot showed that Z-DEVD-FMK decreased the expression of CASP3 and upregulated PARP, the enzyme digestion substrate of caspase-3

correlation analysis between HOXC13 expression and clinical characteristics indicated that expression of HOXC13 is closely linked to primary tumor stage ($P = .010528$) and TNM stage ($P = .031380$) (Table 1). By measuring the mRNA expression of HOXC13 in ESCC tissues from patients at the Nanjing Jinling Hospital, we found that HOXC13 was upregulated in 86.7% of 60 ESCC tissues (Figure 1C), and overexpression of HOXC13 was associated with greater T stage ($P = .0338$), N stage ($P = .0003$) and TNM stage ($P = .0062$) (Figure 1D).

3.2 | Knockdown of HOXC13 inhibits esophageal squamous cell carcinoma proliferation and induces apoptosis in vitro

Confirmed by qRT-PCR and western blot, HOXC13 mRNA level and protein expression were generally higher in ESCC cell lines compared with normal human esophagus cell lines (HET1A), with the ECA109 and TE13 cell line showing the highest expression values (Figure 1E, F). To further investigate the biological function of HOXC13 in ESCC, we conducted two shRNA (sh1 and sh2) to knockdown HOXC13 in ECA109 and TE13 cells. Transfection efficiency was evaluated by qRT-PCR and western blot (Figure 2A,B). Cell Counting Kit-8 (CCK-8) assay, colony formation test and xCELLigence System assay all revealed that knockdown of HOXC13 inhibited proliferation of ECA109 and TE13 cells (Figure 2C-E). The effect of HOXC13 on apoptosis was then evaluated by TUNEL staining. Results indicated that knockdown of HOXC13 significantly induced apoptosis in ECA109 and TE13 cells (Figure 2F).

3.3 | HOXC13 promotes esophageal squamous cell carcinoma proliferation through influencing CASP3

To explore how HOXC13 exerts its oncogenic activity, a list of the 120 genes that had the highest correlation values with HOXC13 were selected from TCGA esophageal carcinoma dataset. Gene ontology pathway analysis showed that genes co-expressed with

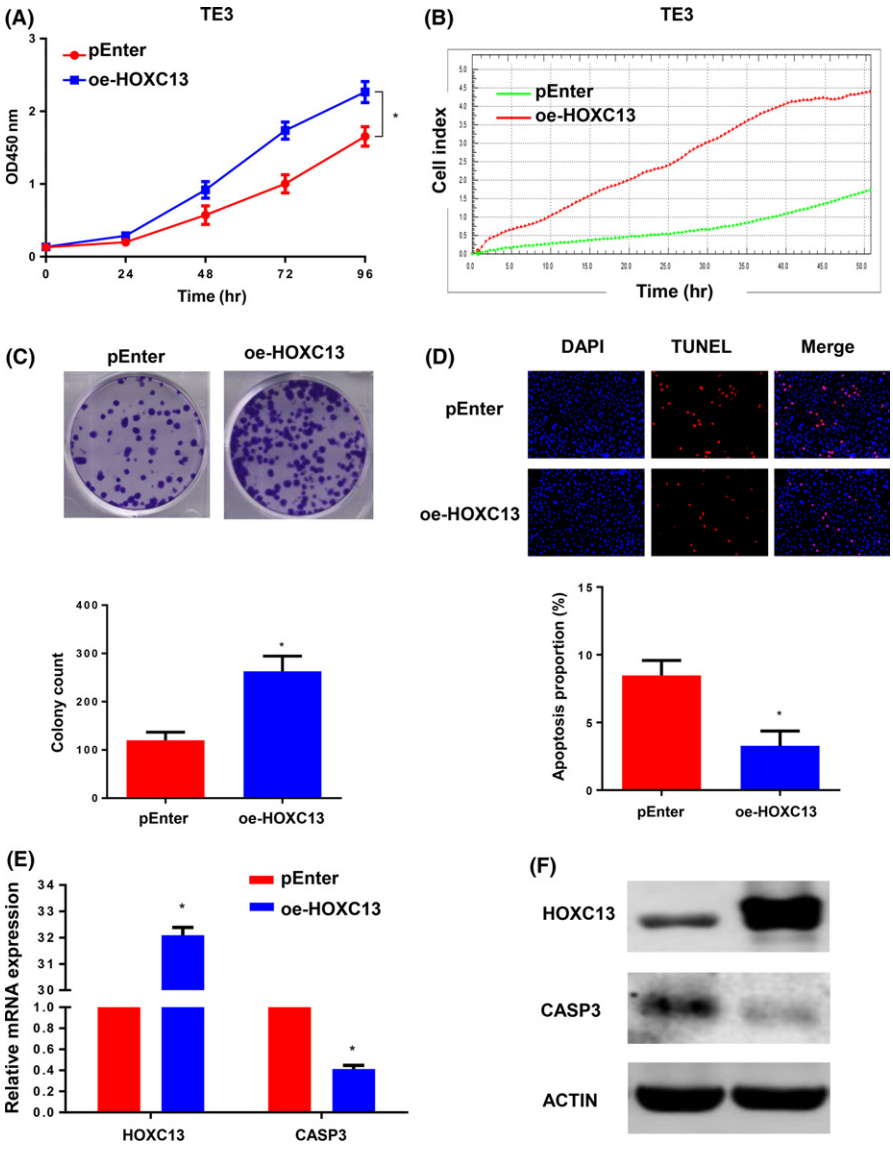

FIGURE 4 Ectopic expression of HOXC13 promotes proliferation of TE3 cells and inhibits apoptosis. A-C, Ectopic expression of HOXC13 promotes proliferation of TE3 cells. D, Ectopic expression of HOXC13 inhibits apoptosis in TE3 cells. E and F, Ectopic expression of HOXC13 downregulates the expression of CASP3

HOXC13 were enriched in the "transcription," "apoptotic process" and "proliferation" pathway (Figure 3A). As HOXC13 might play a pivotal role in apoptosis, we sought to investigate the influence of HOXC13 on apoptosis-related genes. Using qRT-PCR and western blot analysis, we found that expression of CASP3 was significantly upregulated by knockdown of HOXC13 (Figure 3B,C). To clarify whether the effect of HOXC13 on proliferation and apoptosis relied on CASP3, Z-DEVD-FMK, a specific caspase-3 inhibitor, was introduced into sh-HOXC13-treated ECA109 cells. Western blot showed that Z-DEVD-FMK decreased the expression of CASP3 and upregulated PARP, which is the digestion substrate of caspase-3 (Figure 3G). Z-DEVD-FMK could partially reverse the influence of sh-HOXC13 on proliferation and apoptosis in ECA109 cells (Figure 3D-F). Moreover, ectopic expression of HOXC13 promotes proliferation of TE3 cells (Figure 4A-C) and inhibits apoptosis (Figure 4D). The expression of CASP3 was significantly downregulated by overexpression of HOXC13 (Figure 4E,F). Our results demonstrated that HOXC13 might promote ESCC cell proliferation by regulating apoptosis, especially by influencing CASP3.

3.4 | Knockdown of HOXC13 suppresses tumor growth in vivo

Xenograft tumor models were used to assess the oncogenic role of HOXC13 in vivo (Figure 5A). Compared with the control group, tumor volume and tumor weight were smaller in the sh-HOXC13-treated groups (Figure 5B-D). Immunohistochemistry (IHC) analysis revealed that tumors derived from sh-HOXC13 transfected cells showed thicker staining of CASP3 than those in the sh-nc group (Figure 5E).

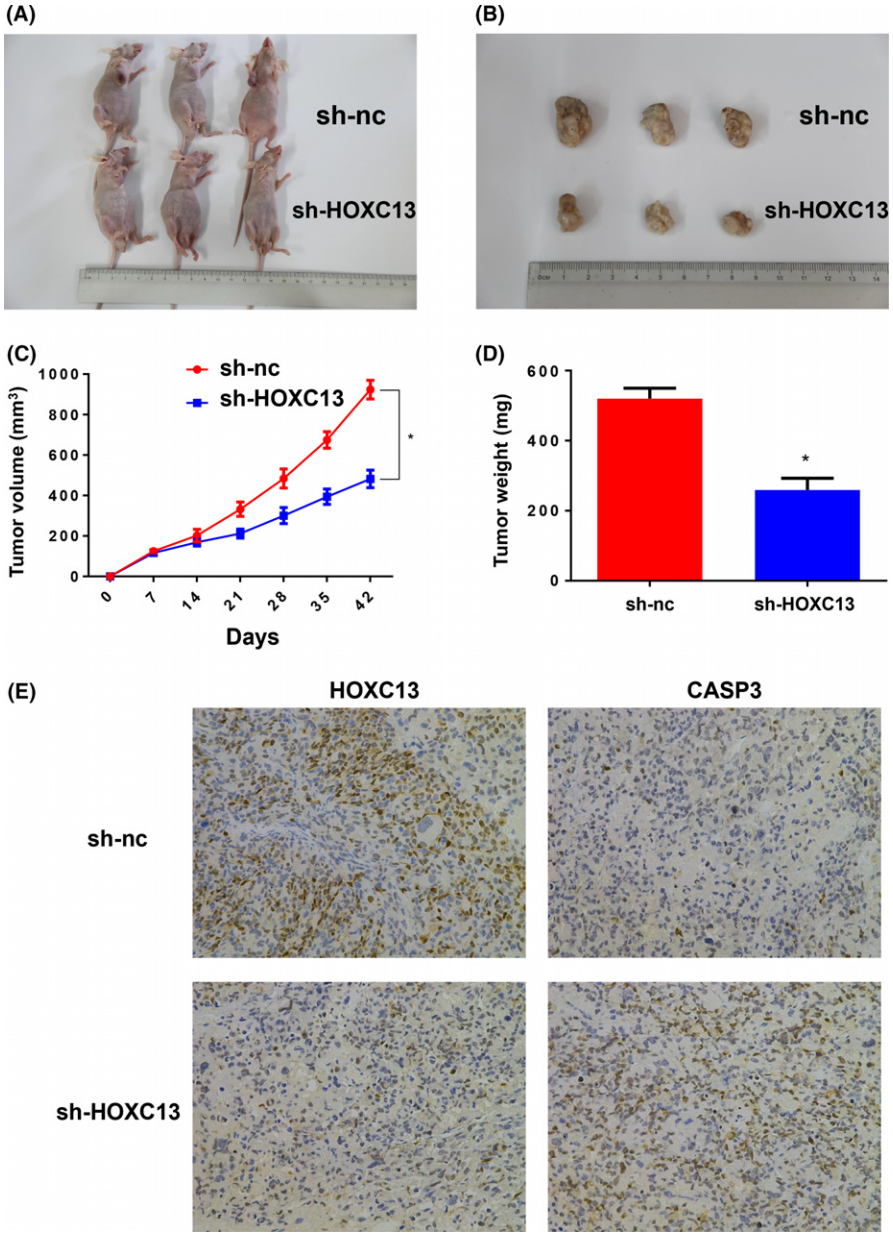

FIGURE 5 Knockdown of HOXC13 inhibits tumor growth in vivo. A,B, Tumor nodules from mice injected with sh-HOXC13 cells were smaller than those injected with sh-nc cells. C,D, Compared with the sh-nc group, the sh-HOXC13 group has reduced tumor volume and weight. E, IHC analysis of xenograft tumors showed that CASP3 staining was thicker in the sh-HOXC13 group

3.5 | HOXC13 represses transcription of CASP3 by directly targeting its promotor region

By analyzing the JASPAR database, we found that HOXC13 has binding sites with the −2000 bp promotor region of CASP3 (Figure 6A). Next, the promoter region containing the HOXC13 binding site was cloned into luciferase reporter vector using genomic DNA and the mutant type was constructed as negative control (Figure 6B). Co-transfections of the luciferase reporter with CMV-HOXC13 expression vectors demonstrated that HOXC13 inhibited transcriptional activity of the CASP3 promoter in HEK293T cells (Figure 6C,D). To determine whether HOXC13 physically bound to the CASP3 promoter region, ChIP was perfomed with anti-HOXC13 antibody and compared to control IgG. Results demonstrated that HOXC13 specifically bound to the CASP3 promoter DNA (Figure 6E,F).

3.6 | MiR-503 inhibits proliferation and induces apoptosis in ECA109 cells through downregulation of HOXC13 by directly targeting its 3′UTR

To identify potential miRNA that target HOXC13, the mirSVR predicted target site scoring method was used. MiR-503 showed great possibility to bind the 3′UTR of HOXC13 (Figure 7A). Luciferase reporter assays demonstrated that miR-503 decreased the luciferase activity of the reporter plasmid carrying the wild-type HOXC13 3′-UTR but not its mutated version (Figure 7B,C). QRT-PCR and western blot also revealed that miR-503 was able to decrease the expression of HOXC13 while increase the expression of CASP3 (Figure 7D). Further investigation showed that miR-503 inhibited proliferation (Figure 7E,F) and induced apoptosis (Figure 7G) in ECA109 cells. The expression of miR-503 in ESCC tissues was measured by qRT-PCR, and results showed that miR-503 was significantly downregulated in ESCC tissues compared with adjacent normal tissues and there is a negative correlation between expression of miR-503 and HOXC13 in ESCC tissues (Figure 7H).

3.7 | MiR-503 inhibits tumor growth in vivo

To confirm the growth-inhibitory effect of miR-503 on ESCC cells in vivo, the subcutaneous growth of tumors derived from ECA109 cells transfected with miR-503 or miR-nc was assessed and xenograft tumors were harvested 6 weeks after injection (Figure 8A,B). Tumor volume and weight were significantly reduced in miR-503-transfected

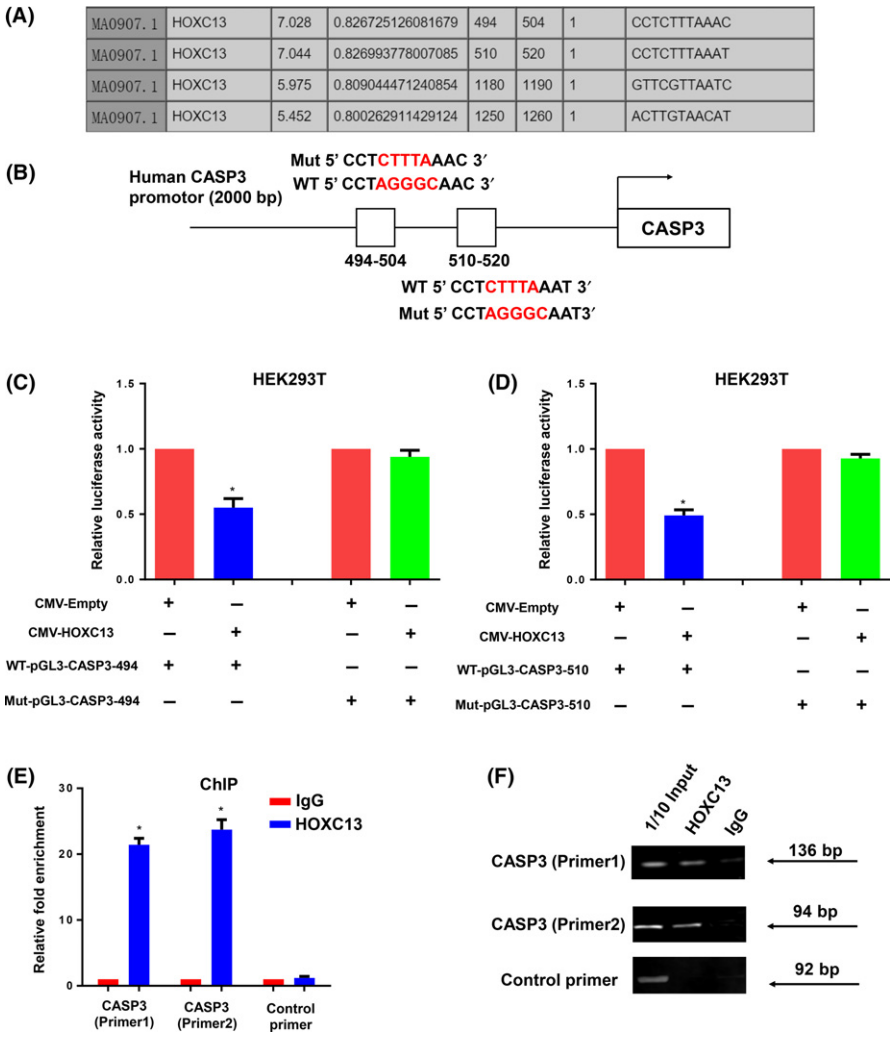

FIGURE 6 HOXC13 directly targets the promotor region of CASP3. A, The JARSPAR database shows that HOXC13 has binding sites with the promotor region of CASP3. B, Schematic illustration of HOXC13 high-score binding site on CASP3 promotor and the mutant CASP3 promotor. C,D, Overexpression of HOXC13 significantly reduced wild type but not mutant CASP3 promoter luciferase activity (CASP3-494, $P = .0004$; CASP3-510, $P < .0001$). E,F, ChIP assays using normal IgG or anti-HOXC13 revealed that HOXC13 directly targets CASP3 promotor region

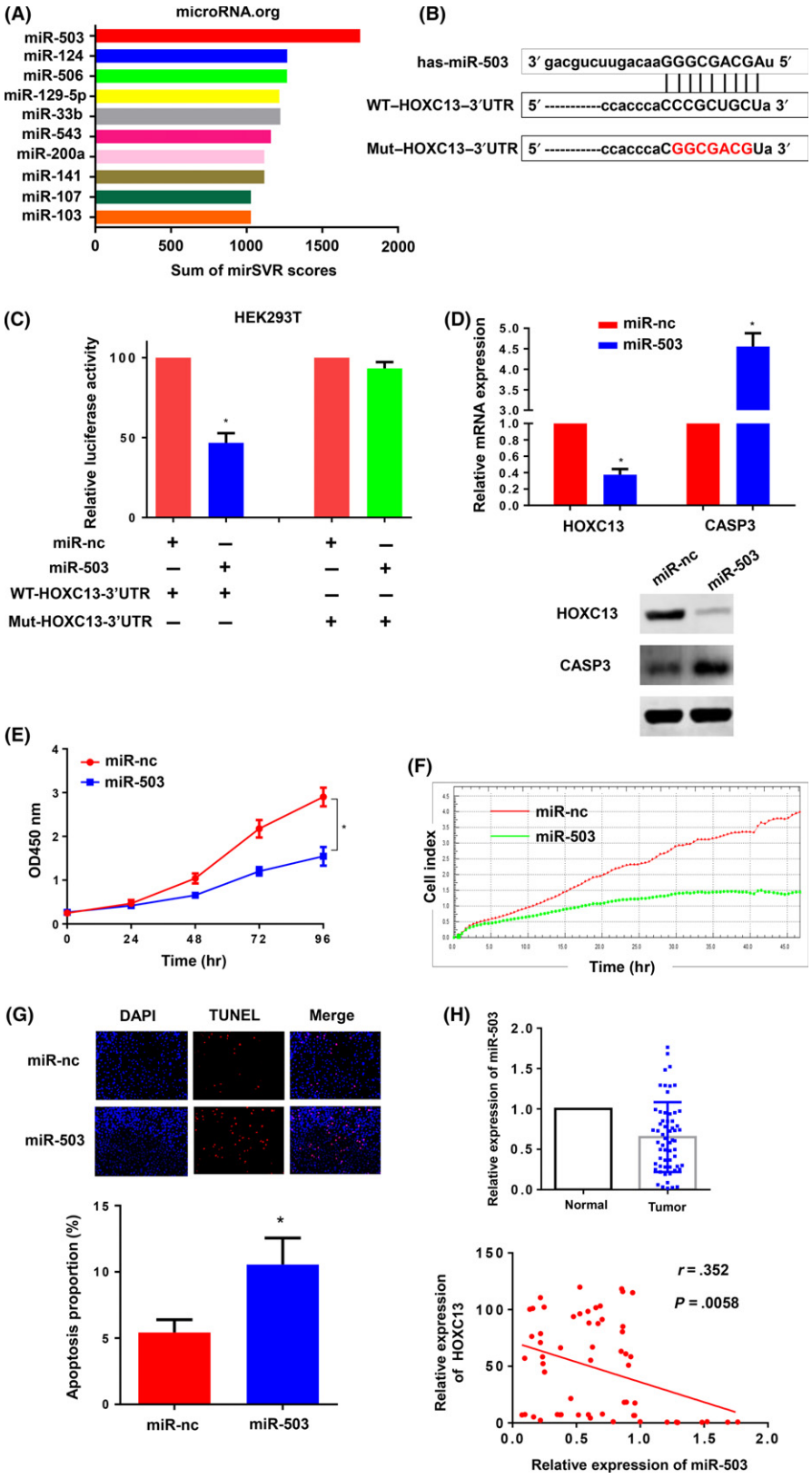

FIGURE 7 MiR-503 directly targets HOXC13 and inhibits proliferation of ECA109 cells. A, MiR-503 showed great possibility to bind the 3′UTR of HOXC13. B, Sequence in HOXC13 3′-UTR that is predicted to be targeted by miR-503 and mutated sequence constructed to prevent targeting. C, Compared with miR-nc, miR-503 decreased the luciferase activity of the reporter plasmid carrying the wild-type HOXC13 3′-UTR ($P = .001$) but not its mutated version. D, Quantitative RT-PCR and western blot showed that miR-503 downregulated the expression of HOXC13 ($P < .0001$) while increased the expression of CASP3 ($P < .0001$). E,F, MiR-503 inhibited the proliferation of ECA109 cells. G, MiR-503 induced apoptosis of ECA109 cells ($P = .0161$). H, MiR-503 was significantly downregulated in ESCC tissues compared with adjacent normal tissues and there is a negative correlation between expression of miR-503 and HOXC13 in ESCC tissues ($n = 60$)

tumors compared with miR-nc (Figure 8C,D). Immunohistochemistry (IHC) analysis showed that HOXC13 protein levels were decreased while CASP3 protein levels were increased in miR-503-transfected tumors (Figure 8E).

4 | DISCUSSION

Esophageal squamous cell carcinoma is the predominant pathological type of esophageal cancer, but the etiology remains poorly

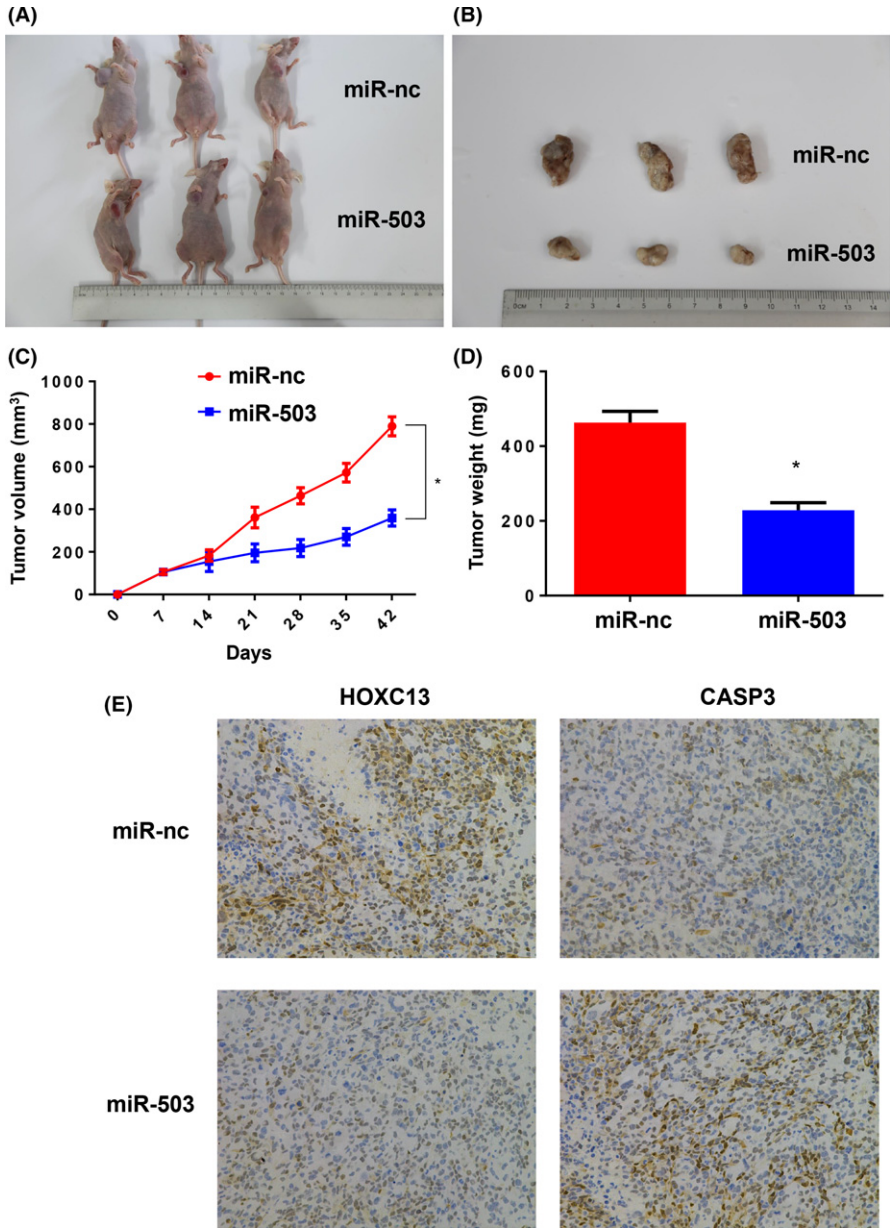

FIGURE 8 MiR-503 inhibits tumor growth in vivo. A,B, Xenograft model in nude mice was used and tumor nodules harvested from miR-503 group were smaller than miR-nc group (C and D). Compared with the miR-nc group, the miR-503 group has reduced tumor volume and weight. E, Immunohistochemistry (IHC) analysis of xenograft tumors showed that HOXC13 protein level was decreased while CASP3 protein level was upregulated in the miR-503 group

understood. Because most patients are diagnosed at a later stage with distant or lymph node metastasis, ESCC has a poor prognosis. Therefore, investigating molecules that play important roles in the initiation and progression of ESCC not only helps to elucidate its pathogenic mechanism but also might provide novel molecular markers and therapeutic targets for the diagnosis and treatment of ESCC.

HOXC13, a member of the homeobox HOXC gene family, has been reported to be overexpressed in human liposarcomas,[12] squamous cell carcinoma,[30] skin tumors[31] and prostate cancer.[32] As a transcription factor, HOXC13 synergistically regulates the expression of Zfp521, which has been identified as a B-cell proto-oncogene causing leukemia.[33] Recent studies show that BMI-1, which is a regulator of HOXC13, and is overexpressed in breast and other cancers, promotes self-renewal of cancer stem-like cells;[34] knockdown of BMI-1 causes cell-cycle arrest, and derepresses p16INK4a in HeLa cells.[35] Moreover, knockdown of HOXC13 affected cell growth, and resulted in cell cycle arrest, in colon cancer.[13] In accordance with these studies, we have uncovered an oncogenic role for HOXC13 in ESCC, by regulation of apoptosis, especially by influencing CASP3.

Apoptosis is a process of programmed cell death that occurs in multicellular organisms and inhibition of apoptosis can result in a number of cancers.[36-38] Apoptosis is generally characterized by phosphatidylserine externalization, depolarization of mitochondrial membrane, caspase-3 activation and DNA fragmentation.[39,40] As one of the most important executioners in the apoptotic process, caspase-3 contains a cysteine residue (Cys-163) and a histidine residue (His-121) that act to stabilize the peptide bond cleavage of the target protein sequence to the carboxy-terminal side of an aspartic acid when it is part of a particular 4-amino acid sequence (Asp-x-x-Asp).[41] Caspase-3 has been identified as the downstream of p53,[42] TLR4-ERK1/2-Fas/FasL,[43] Bcl-2/Bax-Caspase9[44] and JNK/c-Jun,[45]

and plays vital roles in the genesis and development of multiple type of cancers. In our study, we demonstrated that HOXC13 represses transcription of CASP3 by directly targeting its promotor region, thereby exhibiting its oncogenic role in ESCC.

MicroRNA regulate post-transcriptional gene expression by base pairing with complementary sequences in the 3′-UTR of target mRNA, and subsequently inducing mRNA degradation or translational repression.[46] In general, one miRNA appears to be able to regulate several hundred genes; thus, miRNA are involved in a variety of physiological and pathological processes, including the occurrence and development of tumors.[47,48] Our study confirmed that miR-503 directly targets the 3′UTR of HOXC13 and downregulates its expression. MiR-503 has been reported to be closely linked to apoptosis and has been widely studied in cancer. For example, miR-503 induces apoptosis of lung cancer cells by regulating p21 and CDK4 expression;[49] miR-503 inhibits hepatocyte apoptosis through bcl-2 pathway;[50] and miR-503 induces apoptosis and cell-cycle arrest in human ovarian endometriotic stromal cells.[51] Our data confirmed that miR-503 targets 3′UTR of HOXC13 and induces apoptosis in ESCC. Identification of the role of miR-503 in ESCC may lead to the discovery of promising therapeutic targets and prognostic biomarkers in ESCC diagnosis and treatment.

In conclusion, our study showed that HOXC13 expression was significantly elevated in ESCC, and correlated with worse clinical characteristics and poorer prognosis. HOXC13 promoted proliferation and inhibited apoptosis through repressing transcription of CASP3. Moreover, miR-503 was able to inhibit ESCC proliferation by suppressing the expression of HOXC13.

DISCLOSURE STATEMENT

The authors have no conflict of interest to declare.

ORCID

Yi Shen http://orcid.org/0000-0001-9996-646X

REFERENCES

1. Richman DM, Tirumani SH, Hornick JL, et al. Beyond gastric adenocarcinoma: multimodality assessment of common and uncommon gastric neoplasms. *Abdom Radiol (NY)*. 2017;42:124-140.
2. Rustgi AK, El-Serag HB. Esophageal carcinoma. *N Engl J Med*. 2014;371:2499-2509.
3. Pennathur A, Gibson MK, Jobe BA, Luketich JD. Oesophageal carcinoma. *Lancet*. 2013;381:400-412.
4. Pearson JC, Lemons D, McGinnis W. Modulating Hox gene functions during animal body patterning. *Nat Rev Genet*. 2005;6:893-904.
5. Carroll SB. Homeotic genes and the evolution of arthropods and chordates. *Nature*. 1995;376:479-485.
6. Godwin AR, Capecchi MR. Hoxc13 mutant mice lack external hair. *Genes Dev*. 1998;12:11-20.
7. Kulessa H, Turk G, Hogan BL. Inhibition of Bmp signaling affects growth and differentiation in the anagen hair follicle. *EMBO J*. 2000;19:6664-6674.
8. Tkatchenko AV, Visconti RP, Shang L, et al. Overexpression of Hoxc13 in differentiating keratinocytes results in downregulation of a novel hair keratin gene cluster and alopecia. *Development*. 2001;128:1547-1558.
9. Zhong M, Wang J, Gong YB, Li JC, Zhang B, Hou L. Expression of HOXC13 in ameloblastoma. *Zhonghua Kou Qiang Yi Xue Za Zhi*. 2007;42:43-46.
10. Hong YS, Wang J, Liu J, Zhang B, Hou L, Zhong M. Expression of HOX C13 in odontogenic tumors. *Shanghai Kou Qiang Yi Xue*. 2007;16:587-591.
11. Cantile M, Scognamiglio G, Anniciello A, et al. Increased HOXC13 expression in metastatic melanoma progression. *J Transl Med*. 2012;10:91.
12. Cantile M, Galletta F, Franco R, et al. Hyperexpression of HOXC13, located in the 12q13 chromosomal region, in welldifferentiated and dedifferentiated human liposarcomas. *Oncol Rep*. 2013;30:2579-2586.
13. Kasiri S, Ansari KI, Hussain I, Bhan A, Mandal SS. Antisense oligonucleotide mediated knockdown of HOXC13 affects cell growth and induces apoptosis in tumor cells and over expression of HOXC13 induces 3D-colony formation. *RSC Adv*. 2013;3:3260-3269.
14. Bartel DP. MicroRNAs: genomics, biogenesis, mechanism, and function. *Cell*. 2004;116:281-297.
15. Croce CM. Causes and consequences of microRNA dysregulation in cancer. *Nat Rev Genet*. 2009;10:704-714.
16. Ambros V. The functions of animal microRNAs. *Nature*. 2004;431:350-355.
17. Nicoloso MS, Spizzo R, Shimizu M, Rossi S, Calin GA. MicroRNAs–The micro steering wheel of tumour metastases. *Nat Rev Cancer*. 2009;9:293-302.
18. Iorio MV, Croce CM. MicroRNAs in cancer: small molecules with a huge impact. *J Clin Oncol*. 2009;27:5848-5856.
19. Esquela-Kerscher A, Slack FJ. Oncomirs – MicroRNAs with a role in cancer. *Nat Rev Cancer*. 2006;6:259-269.
20. Hu C, Lv L, Peng J, et al. MicroRNA-375 suppresses esophageal cancer cell growth and invasion by repressing metadherin expression. *Oncol Lett*. 2017;13:4769-4775.
21. Tian Y, Luo A, Cai Y, et al. MicroRNA-10b promotes migration and invasion through KLF4 in human esophageal cancer cell lines. *J Biol Chem*. 2010;285:7986-7994.
22. Ma G, Jing C, Li L, et al. MicroRNA-92b represses invasion-metastasis cascade of esophageal squamous cell carcinoma. *Oncotarget*. 2016;7:20209-20222.
23. Mathe EA, Nguyen GH, Bowman ED, et al. MicroRNA expression in squamous cell carcinoma and adenocarcinoma of the esophagus: associations with survival. *Clin Cancer Res*. 2009;15:6192-6200.
24. Garzon R, Marcucci G, Croce CM. Targeting microRNAs in cancer: rationale, strategies and challenges. *Nat Rev Drug Discov*. 2010;9:775-789.
25. Goldman M, Craft B, Swatloski T, et al. The UCSC cancer genomics browser: update 2015. *Nucleic Acids Res*. 2015;43:D812-D817.
26. Gao J, Aksoy BA, Dogrusoz U, et al. Integrative analysis of complex cancer genomics and clinical profiles using the cBioPortal. *Sci Signal* 2013;6:pl1.
27. Vastrik I, D'Eustachio P, Schmidt E, et al. Reactome: a knowledge base of biologic pathways and processes. *Genome Biol*. 2007;8:R39.
28. Mathelier A, Fornes O, Arenillas DJ, et al. JASPAR 2016: a major expansion and update of the open-access database of transcription factor binding profiles. *Nucleic Acids Res*. 2016;44:D110-D115.
29. Betel D, Koppal A, Agius P, Sander C, Leslie C. Comprehensive modeling of microRNA targets predicts functional non-conserved and non-canonical sites. *Genome Biol*. 2010;11:R90.
30. Marcinkiewicz KM, Gudas LJ. Altered histone mark deposition and DNA methylation at homeobox genes in human oral squamous cell carcinoma. *J Cell Physiol*. 2014;229:1405-1416.

31. Battistella M, Carlson JA, Osio A, Langbein L, Cribier B. Skin tumors with matrical differentiation: lessons from hair keratins, beta-catenin and PHLDA-1 expression. *J Cutan Pathol*. 2014;41:427-436.
32. Komisarof J, McCall M, Newman L, et al. A four gene signature predictive of recurrent prostate cancer. *Oncotarget*. 2017;8:3430-3440.
33. Yu M, Al-Dallal S, Al-Haj L, et al. Transcriptional regulation of the proto-oncogene Zfp521 by SPI1 (PU.1) and HOXC13. *Genesis*. 2016;54:519-533.
34. Hiraki M, Maeda T, Bouillez A, et al. MUC1-C activates BMI1 in human cancer cells. *Oncogene*. 2017;36:2791-2801.
35. Chen F, Li Y, Wang L, Hu L. Knockdown of BMI-1 causes cell-cycle arrest and derepresses p16INK4a, HOXA9 and HOXC13 mRNA expression in HeLa cells. *Med Oncol*. 2011;28:1201-1209.
36. Chen G, Zhang B, Xu H, et al. Suppression of Sirt1 sensitizes lung cancer cells to WEE1 inhibitor MK-1775-induced DNA damage and apoptosis. *Oncogene*. 2017:1-10.
37. Tu YS, He J, Liu H, et al. The imipridone ONC201 induces apoptosis and overcomes chemotherapy resistance by up-regulation of Bim in multiple myeloma. *Neoplasia*. 2017;19:772-780.
38. Dhivya R, Ranjani J, Bowen PK, Rajendhran J, Mayandi J, Annaraj J. Biocompatible curcumin loaded PMMA-PEG/ZnO nanocomposite induce apoptosis and cytotoxicity in human gastric cancer cells. *Mater Sci Eng C Mater Biol Appl*. 2017;80:59-68.
39. Jellinger KA. Challenges in neuronal apoptosis. *Curr Alzheimer Res*. 2006;3:377-391.
40. Bialostozky D, Rodriguez-Diez G, Zazueta C. Apoptosis detection in cardiovascular diseases through nuclear cardiology SPECT images. *Arch Cardiol Mex*. 2008;78:217-228.
41. Feeney B, Pop C, Swartz P, Mattos C, Clark AC. Role of loop bundle hydrogen bonds in the maturation and activity of (Pro)caspase-3. *Biochemistry*. 2006;45:13249-13263.
42. Liu C, Vojnovic D, Kochevar IE, Jurkunas UV. UV-A irradiation activates Nrf2-regulated antioxidant defense and induces p53/caspase3-dependent apoptosis in corneal endothelial cells. *Invest Ophthalmol Vis Sci*. 2016;57:2319-2327.
43. Tian Y, Wang J, Wang W, et al. Mesenchymal stem cells improve mouse non-heart-beating liver graft survival by inhibiting Kupffer cell apoptosis via TLR4-ERK1/2-Fas/FasL-caspase3 pathway regulation. *Stem Cell Res Ther*. 2016;7:157.
44. Wu R, Tang S, Wang M, Xu X, Yao C, Wang S. MicroRNA-497 induces apoptosis and suppresses proliferation via the bcl-2/bax-caspase9–caspase3 pathway and cyclin D2 protein in HUVECs. *PLoS ONE*. 2016;11:e0167052.
45. Sun WJ, Huang H, He B, et al. Romidepsin induces G2/M phase arrest via Erk/cdc25C/cdc2/cyclinB pathway and apoptosis induction through JNK/c-Jun/caspase3 pathway in hepatocellular carcinoma cells. *Biochem Pharmacol*. 2017;127:90-100.
46. Bartel DP. MicroRNAs: target recognition and regulatory functions. *Cell*. 2009;136:215-233.
47. Liu CG, Calin GA, Volinia S, Croce CM. MicroRNA expression profiling using microarrays. *Nat Protoc*. 2008;3:563-578.
48. Singh R, Ramasubramanian B, Kanji S, Chakraborty AR, Haque SJ, Chakravarti A. Circulating microRNAs in cancer: hope or hype? *Cancer Lett*. 2016;381:113-121.
49. Sun Y, Li L, Xing S, et al. miR-503-3p induces apoptosis of lung cancer cells by regulating p21 and CDK4 expression. *Cancer Biomark*. 2017, 1-12.
50. Xie Z, Xiao Z, Wang F. Hepatitis C Virus nonstructural 5A protein (HCV-NS5A) inhibits hepatocyte apoptosis through the NF-kappab/miR-503/bcl-2 pathway. *Mol Cells*. 2017;40:202-210.
51. Hirakawa T, Nasu K, Abe W, et al. miR-503, a microRNA epigenetically repressed in endometriosis, induces apoptosis and cell-cycle arrest and inhibits cell proliferation, angiogenesis, and contractility of human ovarian endometriotic stromal cells. *Hum Reprod*. 2016;31:2587-2597.

SUPPORTING INFORMATION

Additional Supporting Information may be found online in the supporting information tab for this article.

How to cite this article: Luo J, Wang Z, Huang J, et al. HOXC13 promotes proliferation of esophageal squamous cell carcinoma via repressing transcription of CASP3. *Cancer Sci*. 2018;109:317–329. https://doi.org/10.1111/cas.13453